1. Figure legends for the supplementary table and figures.

Table S1: Complete Prolucid (Sequest) protein database search results after DTASelect data filtering for GluA2 (A2), GluK2 (K2), and control (IgG) rat purifications (Related to Table 1)

A roadmap for navigating this table: The Excel table contains the detailed and complete proteomic analysis results as **11 tabs**. Visiting the **compare_ALL** tab first is recommended for readers who wish to quickly view the complete list of identified proteins. The other tabs contain detailed information about the peptides, spectra, and statistical values.

The **compare_ALL** tab lists every protein identified in all the considered experiments including the duplicate experiment (indicated as different trials at the top of the column) and IgG control. The semi-quantitative spectral counts are indicated. The proteins in red were found in the IgG control purification and excluded.

The database used for searching is contained in the name of each tab. For example, **R2_Rat** was searched against rat protein database and **R2_HumanMouseRat** was searched against a concatenated database consisting of the human-mouse-rat protein databases.

GluA2 affinity purification results are presented in 4 tabs; **R2_Rat** and **R2_HumanMouseRat** contain DTASelect results and the other two tabs suffixed with **summary** contain their summary. Similarly, GluK2 affinity purification results are presented in 4 tabs; **R6_Rat** and **R6_HumanMouseRat** tabs contain DTASelect results and the other two tabs suffixed with **summary** contain their summary. The IgG control affinity purification results are represented in 2 tabs; **IgG_RatDB** contains DTASelect results and **IgG_Rat_summary** contains its summary.

Each DTASelect result is composed of a header (containing the search and filtering parameters), main data, and dataset summaries at the bottom. Specifically, detailed spectra, peptide, protein, and dataset statics are indicated in the DTASelect results; the exact measured FDR, based on reverse database hits at the protein (<1% for each search), peptide, and spectra level can be found at the bottom of the search result. Likewise, each corresponding **summary** tab provides collapsed view by extracting from DTASelect results the protein IPI number, Sequence % coverage, Spectrum counts, and Peptide counts.

Figure S1. Claudin homologue GSG1L is a candidate auxiliary subunit of human AMPA-Rs (Related to Figure 1)

A. LC-MS/MS analysis identified GSG1L protein from human GluA2 purification. Shown are protein identification summaries for GluA2 and GSG1. Note, two human GSG1L isoforms were identified by the same peptides thus either isoforms, or both could be present.

B. Detailed peptide statistics for GSG1L protein identification. Three fully tryptic peptides were identified with confident Xcorr, DeltaCN, and precursor ppm scores as indicated.

C. MS/MS spectrum for the human GSG1L peptide R.NFHTGIWYSCEEELSGLGEK.C (+2 charge).

D. Multiple sequence alignment of rat GSG1L, GSG1, and TARPs (gamma-2, 3, 4, and 8) by CLUSTALW. The predicted location of the transmembrane domains are boxed and indicated as TM1-4. The antigen peptides used to generate anti-

GSG1L antibodies are indicated by red boxes. Residues with similar chemical properties are color-coded.

Figure S2. GSG1L interacts with AMPA-R subunits (Related to Figure 1)

A1. HEK cells were transfected with plasmids that express the proteins indicated at the top of each lane. Immunoprecipitation was conducted using anti-GluA2CT (αA2) antibody. Western blots of the input and immunoprecipitation (IP) are shown. Membranes were probed with antibodies indicated in the right. EGFP was used as negative control.

A2. HEK cells were transfected with plasmids that express the proteins indicated at the top of each lane. Immunoprecipitation was conducted using anti-GluK2CT antibody. Western blots of the input and immunoprecipitation (IP) are shown. Membranes were probed with antibodies indicated in the right. EGFP was used as negative control.

Molecular weight markers in this figure are indicated on the left (kDa).

C. Colocalization of GSG1L and GluA2 in HEK cells. Confocal images HEK cells transiently cotransfected with plasmids driving the expression of GSG1L (ctHA indicates an HA tag at the C-terminal) and GluA2. Scale bar = 10μm (upper panels) and 0.5 μm (lower panels). The two proteins co-localize at the cell surface. The strong perinuclear staining of GSG1L is observed when transient transfection of plasmids is used but is absent when expressed moderately using DOX inducible expression system in combination with stable cell lines (Data shown in the main Figure 2C).

Figure S3. Functional modulation of AMPA-R by GSG1L (Related to Figure 2)

A. Cartoon depicting the DOX inducible expression of GluA2 and constitutive expression of stargazin (stg) or GSG1L. Specifically, these cells constitutively express (stg or GSG1L)-IRES-mCherry module under the control of constitutive elongation factor promoter, and a reverse Tet transcriptional element (rTet). The latter enhances transcription of the GluA2*flip*-FLAG transgene from the minimal CMV promoter when the drug doxycycline (DOX) is present in the cell media. Na butyrate was also added together with DOX to enhance protein induction.

B. Western blot showing the time course of GluA2 expression after DOX induction in the indicated stable cell lines. Top: TetON GluA2flipFLAG#4 cell line that DOX dependently express GluA2. Bottom: TetON GluA2flipFLAG pBOSS-GSG1LntHA#25 cell line that DOX dependently express GluA2 and constitutively express HA tagged GSG1L. Membranes were probed with antibodies indicated at the bottom. We also observed that GSG1L accelerates glycosylation of GluA2 (Fig S3B). This effect was not observed in the case of stargazin (Shanks et al., 2010) and is specific to GSG1L.

C. The trajectory of the cytotoxicity after inducing GluA2 expression is shown by the DIC images of the cells taken on different days in pBOSS-stg-IRIS-mCherry#7 (C1), TetON GluA2flipFLAG pBOSS-GSG1LntHA#25 (C2), and TetON GluA2flipFLAG (C3) cell lines. The cells on the left column were untreated (No drugs), whereas the other columns were treated with DOX+Na butyrate with (+NBQX) or without 30 µM NBQX. Scale bar = 200 µm. Insets are representative enlarged views. The time course of cell death however was slower when GSG1L was present instead of stargazin (complete cell death in 2 days for stargazin vs. 3 days for GSG1L), indicating possible differences between stargazin and GSG1L in modulating AMPA-R function.

2. Detailed Methods

Antibodies

Anti-GluA2CT antibody and ProteinA sepharose beads conjugated with this antibody were described previously (Nakagawa et al., 2005). Anti-GluK2CT antibody was affinity purified from rabbit serum obtained from rabbits that were immunized with the following peptide antigen, CVKTEEVINMHTFNDRRLPGKEMTA. CNBr-activated Sepharose beads (GE Healthcare) were conjugated with a GST fusion protein that contains the antigen sequence, and used for affinity purification column. Normal rabbit IgG was purchased from Pierce. The purified antibody was covalently conjugated with ProteinA Sepharose using DMP (Pierce).

The Lp1, Ct1, and Ct2, peptide antigens for anti-GSG1L antibodies were, RFHTGIWYSCEEELGGPGEKC, CRSSAHEAAELNRQCWVLGHWV, and CKVFEQGYREEPTFIDPEAIKYFR respectively, and were synthesized. Each antigen was conjugated to maleimide activated KLH via cysteine and used to immunize rabbits (Genscript). The antibodies were affinity purified using columns conjugated via CNBr, purified GST fusion proteins expressed in bacteria. The amino acid sequences of GSG1L fused to GST using pGEX4T-1 plasmid were GST-Lp1: TYWCQGTQRVPKPGCGQGGGANCPNSGANATANSTAAPVAASPAGAPYSW EAGDERFQLRRFHTGIWYSCEEELGGPGEKCRSFIDLAPASEK, GST-Ct3: GDSWPRSSAHEAAELNRQCWVLGHWV , and GST-Ct8: TKTVIEFRHKRKVFEQGYREEPTFIDPEAIKYFRERIEKGDVSEEED, respectively. The antigens are underlined.

Purification of AMPA and KA-Rs from rat brain

Using Protein A Sepharose beads covalently conjugated with antibodies that specifically recognize GluA2 andGluK2, we purified native AMPA-R and KA-R complexes from CHAPS extracted brain membranes obtained from P15 rats that

were anesthetized with isofluorane and decapitated. Protocols approved by IACUC of UCSD were followed. Beads conjugated with normal rabbit IgG were prepared similarly and used during purification as negative control. The adopted purification protocol was similar to what was used for purifying native AMPA-R complexes for EM studies (Nakagawa et al., 2005). Rat brains were homogenized in 20 mM HEPES, pH 7.4, 320 mM sucrose, 5 mM EDTA, 5 mM EGTA, 30 µM NBQX supplemented with protease inhibitors (1 mM PMSF, 10 µg/ml aprotinin, 10 µg/ml leupetin, 1 µg/ml pepstatin, and 500 µM benzamidine). Supernatant was obtained by centrifuging the homogenate at 3,000 g for 15 min was further spun at 38,400 g for 15 min to obtain a membrane pellet (P2 fraction). P2 was resuspended in SB1 (20 mM HEPES, pH 7.4, 1 M KI, 5 mM EDTA, 5 mM EGTA, and 30 µM NBQX) and membranes were collected by centrifugation. Membranes were further washed with WB (20 mM HEPES, pH 7.4, 5 mM EDTA, 5 mM EGTA, 30 µM NBQX) to remove KI. Finally, membranes were solublized in RB (20 mM HEPES, pH 7.4, 100 mM NaCl, 5 mM EDTA, 5 mM EGTA, 1 % CHAPS, 30 µM NBQX, with protease inhibitors) for 3hr with gentle stirring at 4 ^{o}C and ultracentrifuged at 100,000 g to remove insoluble material. The final supernatant was applied to appropriate antibody affinity column (0.25 ml bed volume, antibody concentration 2 mg/ml). After washing the column with 3 ml of sample buffer, bound proteins were eluted with 100 mM glycine pH 2.5, 1% CHAPS and each eluted fractions were immediately mixed with 1/10 volume of 1M TrisHCl pH8.5. The affinity purified material was then precipitated with 15% TCA (trichloroacetic acid). The experiment was duplicated using smaller number of rat brains (at approximately 1/2 scale). The duplicate results are summarized in the Compare_all tab. For experiments shown in Figure 1D, the column elution was conducted using 20 mM HEPES, pH 7.4, 150 mM NaCl, 5 mM EDTA, 5 mM EGTA, 1% CHAPS, 30 µM NBQX, 0.5 µg/ml GluA2 C-terminal epitope peptide (GYNVYGIESVKI).

Purification of AMPA-R from human brain

Human brain (cortex) was obtained through the National Disease Research Interchange (NDRI), Researcher: Yates (code YAJ2), TSRI: IRB-11-5719. The antigen of the antibody against GluA2 is conserved in rat and human. GluA2 from human cortex was immunoaffinity purified using identical purification protocol used to purify rat GluA2.

Mass spectrometry

Sample Preparation: TCA precipitate was resuspended in 8M urea. Next the extracts were processed with ProteasMAX (Promega, Madison, WI, USA) per the manufacturer's instruction. The samples were subsequently reduced by 20 minute incubation with 5mM TCEP (*tris*(2 carboxyethyl)phosphine) at room temperature and alkylated in the dark by treatment with 10mM Iodoacetamide for 20 additional minutes. The proteins were digested over-night at 37 degrees with Sequencing Grade Modified Trypsin (Promega, Madison, WI, USA) and the reaction was stopped by acidification.

Multidimensional Protein Identification Technology (MudPIT) and LTQ and LTQ Orbitrap Mass Spectromtery: The protein digest was pressure-loaded onto a 250--µm i.d capillary packed with 2.5cm of 10-µm *Jupiter C18 resin* (Phenomenex, Torrance, CA, USA) followed by an additional 2.5cm of 5-µm Partisphere strong cation exchanger (Whatman, Clifton, NJ). The column was washed with buffer containing 95% water, 5% acetonitrile, and 0.1% formic acid. After washing, a 100--µm i.d capillary with a 5-µm pulled tip packed with 15 cm 4-µm *Jupiter C18 resin* (Phenomenex, Torrance, CA, USA) was attached to the filter union and the entire split-column (desalting column–filter union–analytical column) was placed inline with an Agilent 1100 quaternary HPLC (Palo Alto, CA) and analyzed using a modified 5-step separation described previously (Washburn et al., 2001). The buffer solutions used were 5% acetonitrile/0.1% formic acid (buffer A), 80% acetonitrile/0.1% formic acid (buffer B), and 500 mM ammonium acetate/5% acetonitrile/0.1% formic acid (buffer C). Step 1 consisted of a 75 min gradient from 0-100% buffer B. Steps 2-5 had a similar

profile except 3 min of 100% buffer A, 5 min of X% buffer C, a 10 min gradient from 0-15% buffer B, and a 105 min gradient from 10-55% buffer B (except for step 5 which %B was increased from 10% to 100%). The 5 min buffer C percentages (X) were 10, 40, 60, 100% respectively for the 5-step analysis. As peptides eluted from the microcapillary column, they were electrosprayed directly into an LTQ mass spectrometer (ThermoFinnigan, Palo Alto, CA).

For LTQ analysis (Rat GluA2, GluK2 and normal IgG): As peptides eluted from the microcapillary column, they were electrosprayed directly into an LTQ 2-dimensional ion trap mass spectrometer (ThermoFinnigan, Palo Alto, CA) with the application of a distal 2.4 kV spray voltage. A cycle of one full-scan mass spectrum (400-1400 m/z) followed by 7 data-dependent MS/MS spectra at a 35% normalized collision energy was repeated continuously throughout each step of the multidimensional separation. Application of mass spectrometer scan functions and HPLC solvent gradients were controlled by the Xcalibur datasystem.

For LTQ velos Orbitrap analysis (Human GluA2): A seven step MudPIT was employed (10, 30, 50, 70, 90, 100% buffer C). A cycle of one full-scan mass spectrum (400-1800 m/z) at a resolution of 60,000 followed by 20 data dependent MS/MS spectra at a 35% normalized collision energy was repeated continuously throughout each step of the multidimensional separation. Maximum ion accumulation times were set to 500ms for survey MS scans and to 100ms for MS2 scans. Charge state rejection was set to omit singly charged ion species and ions for which a charge state could not be determined for MS/MS. Minimal signal for fragmentation was set to 1000. Dynamic exclusion was enabled with a repeat count:1, duration:20.00S, list size:300, exclusion duration 30.00S, exclusion mass with high/low: 1.5m/z. Application of mass spectrometer scan functions and HPLC solvent gradients were controlled by the Xcaliber data system.

Analysis of Tandem Mass Spectra

Protein identification and quantification analysis were done with Integrated Proteomics Pipeline (IP2, Integrated Proteomics Applications, Inc. San Diego, CA) using ProLuCID, DTASelect2 and Census. Tandem mass spectra were extracted into ms1 and ms2 files (McDonald et al., 2004) from raw files using RawExtract 1.9.9 (http://fields.scripps.edu/downloads.php) and were searched against IPI rat protein database (For Rat searches:version 3.0, released on 06-28-2007; For Shisa, SynDIG1, and Neto1 identifications from Rat purifications: concatenated human-mouse-rat version 3.71, released_03-24-2010; For Human GluR searches version 3.57, released 01-01-2009)) plus sequences of known contaminants such as keratin and porcine trypsin concatenated to a decoy database in which the sequence for each entry in the original database was reversed (Peng et al., 2003) using ProLuCID/Sequest (Eng J, 1994). LTQ data was searched with 3000.0 milli-amu precursor tolerance, for LTQ velos Orbitrap data we used 50.0ppm tolerance for precursor ions and the fragment ions for both searches were restricted to a 600.0ppm tolerance.

All searches were parallelized (Sadygov et al., 2002) and performed on The Scripps Research Institute's garibaldi 64-bit LINUX cluster with 2848 cores. Search space included all fully- and half-tryptic peptide candidates with no missed cleavages restrictions. Carbamidomethylation (+57.02146) of cysteine was considered as a static modification, we require 2 peptides per protein and at least one trypitic terminus for each peptide identification. The ProLuCID search results were assembled and filtered using the DTASelect program (version 2.0) (Cociorva et al., 2007; Tabb et al., 2002) with false discovery rate (FDR) of 0.05, under such filtering conditions, the estimated false discovery rate was below 1% at the protein level in all analysis.

The RAW files and parameter files will be publically available at http://fields.scripps.edu/published/iGluR upon publication.

Plasmid DNA Construction

Rat GSG1L cDNA was synthesized (Genscript) based on genbank entry XP_574558.2. An HA tag in the N-terminus (ntHA) or C-terminus (ctHA) was introduced using PCR. These fragment were subcloned between EcoRI and SalI sites of pTREt vector (Clontech). To generate pBOSS-GSG1LctHA-IRES-mCherry, EcoRI-SalI fragment was first cloned into pIRES-mCherry vector (Clontech), then the EcoRI-NotI fragment containing GSG1L was subcloned into modified pBOSS vector (Shanks et al., 2010). pBOSS vector drives the expression of a gene of interest using an elongation factor promoter. For the surface labeling experiments, a GSG1L construct was created that has an HA tag in the extracellualr loop1 (AAPVAA*SPAGAPY, where HA tag was inserted at the asterisk). All DNA fragments created by PCR were sequence verified.

Co-immunoprecipitation of GSG1L-HA proteins with iGluRs in HEK cells

Co-immunoprecipitation of iGluRs with GSG1L (Figure 1D1 and 2). TetON HEK cells (Clontech) were used to create stable cell lines. TetON-GluA2flipFLAG#4 (a stable TetON HEK cell line that DOX dependently express GluA2flip-FLAG) and TetON-GluK2#16 cells (a stable HEK cell line that DOX dependently express GluK2-FLAG) were transfected with pTREt-GSG1LctHA, pTREtB-HA-Neto2 or pTREtB-EGFP constructs using calcium phosphate methods and grown for 12 hours with 30µM NBQX and 1mM kynurenic acid. Protein expression was then induced with 7.5µg/ml DOX and 1mM Na-butyrate. After 24 hours cells were washed with cold D-PBS twice and resuspended in 900ul of buffer containing 50mM Na-HEPES, 85mM NaCl, 15mM KCl and protease inhibitors (1 mM PMSF, 10 µg/ml aprotinin, 10 µg/ml leupetin, 1 µg/ml pepstatin, and 500 µM benzamidine). Membranes were lysed with 0.25% DDM (Anatrace, SOL-grade) in the above buffer for 1.5 hours at 4 ^{o}C, ultracentrifuged at 35 krpm (Beckman, TLA-55) for 15 minutes at 4 ^{o}C. The supernatant was incubated with HA antibody (HA.11 Covance) for about 15 hours. 30 µl of protein A sepharose beads were incubated for 3 hours. After washing the beads 3 times in buffer, protein was eluted off the beads by boiling with SDS-PAGE loading buffer containing 100 mM

DTT. Western blotting was done using anti-GluA2CT, anti-GluK2CT and anti-HA antibody (HA.11, Covance).

Co-immunoprecipitation of GSG1L with iGluR subunits (Figure 1E1 and 2). TetON HEK cells were used instead of receptor stable cell lines. The following combinations were transfected: pTREt-GluA2flipFLAG/pTREt-GSG1LctHA, pTREt-GluA2flipFLAG/pTREtBa-EGFP, pTREt-GluK2/pTREt-GSG1LctHA, pTREt-GluK2/pTREtBa-EGFP and 2 plates of pTREtBa-EGFP/pTREt-GSG1LctHA. Immunoprecipications were conducted as above except anti-GluA2CT or anti-GluK2CT were used as IP antibodies.

Co-immunoprecipitation of GSG1L with GluA1 subunit (Figure 1G). TetON HEK cells were used. The following plasmids were transfected: pTREt-GSG1LctHA, pTREt-Venus-HA, pTREt-GluA1-FLAG, and pTREt-GluA2flipFLAG. The FLAG tag is located at the very C-terminal of GluA1 and 2.

Surface labeling of GluA2 in HEK cells

TetON HEK cells (Clontech) were plated on poly-L-lysine coated glass coverslips. Two days later, cells were co-transfected with pTREt-GluA2flop-FLAG and one of pTREt-GSG1LctHA, pTREt-GSG1LntHA, pTREtBa-EGFP or pTREt-Stargazin and cultured in the presence of 1mM kynurenic acid and 30µM NBQX to block the cell toxicity. The next day, transgenes were induced by the application of 7.5µg/ml DOX and 1mM sodium butyrate. Sodium butyrate is used to relax the chromatin structure and enhance protein expression of the protein of interest from DOX inducible promoter. 24 hours later, surface GluA2 were live labeled using anti-GluA2-NTD antibody (1:100, Chemicon MAB397) for 15 min in 5%CO_2 incubator at 37^{o}C. After washing, cells were fixed with 4% formaldehyde in 0.1M phosphate buffer (pH7.4) for 7min. Goat anti-mouse IgG conjugated with Alexa568 (Invitrogen, Molecular Probes) was used to visualize the labeled GluA2. Images of each condition were recorded using a CCD camera

(Hamamatsu photonics, ORCA) mounted on an epifluorescent microscope (Olympus, 10x objective lens) using the identical settings throughout the experiment.

Generation of stable TetON HEK cell line that DOX dependently expresses GluA2 and constitutively expresses GSG1L

To generate the cell line, we took the same approach as previously described (Shanks et al., 2010), but we co-transfected pBOSS-GSG1LntHA-IRES mCherry with Zeocin resistance gene encoding plasmid (pCMVZeo, Invitrogen) into TetON-GluA2flipFLAG#4 cell line.

Generation of stable TetON HEK cell line that DOX dependently expresses GluA2 and GSG1L

GSG1LntHA and GluA2-FLAG were subcloned into dual expression plasmid modified from pTREt (Clontech) described previously (Farina et al., 2011). This plasmid was co-transfected with hygromycin resistance gene encoding plasmid into TetON HEK cell (Clontech).

Cell death assay using stable cell lines

Stable cell lines, TetON-GluA2flipFLAG#4, TetON-GluA2flipFLAG-pBOSS-stargazin-IRESmCherry#7, TetON-GluA2flipFLAG-pBOSS-GSG1LntHA-IRESmCherry#25 were replated in the culture media without NBQX at sparse density in 3 wells. Two days after the plating, 2 wells were induced with 7.5 µg/ml DOX and 1mM Na butyrate, one of them was supplemented with 30µM NBQX and 1 well was left as control without drug (no-drug). Approximately 0, 24, 48 and 72 hours after the induction, DIC images of cells were taken.

Time course experiment

TetON-GluA2flipFLAG#4, TetON-GluA2flipFLAG-pBOSS-GSG1LntHA-IRESmCherry#25 cells were plated on 6 well plates at the density of 1.5x10^6 cells / well. The next day, 4 wells of cells were induced with 7.5µg/ml DOX and

1mM Na butyrate. 6, 12, 18 and 24 hours later, 1 well of each line was washed using 1ml PBS once, harvested in 1ml PBS, spin down at 4^{o}C, supernatant removed, and flash frozen in liquid N2. At 24 hours time point, non-induced cells were also harvested. Frozen pellets were resuspended in 400µl of PBS and 200ul of 4xDTT SDS-PAGE sample buffer was added. Samples were loaded on western blotting using GluA2CT and anti-HA antibody (Covance).

Neuron transfection and surface labeling

Embryonic day 18 cortical culture and surface labeling were conducted as previously described (Shanks et al., 2010, Sala et al., 2003) with slight modifications. Briefly, the cortex without the hippocampus was dissected and culture media was supplemented with 1.5%FCS. 16DIV cortical neurons were transfected with pTREt-GSG1L-surface HA tag and pTetON-Advanced plasmids (at a 9:1 ratio) using calcium phosphate methods. At 18 DIV, cells were induced with 5µg/ml DOX for 24~48 hours. Cells were labeled using anti-HA monoclonal antibody (1:1000, Covance) or anti-HA polyclonal (1:50, Santa Cruz) followed by rabbit GluA2CT (1:200), anti-GluA1CT (1:50) (Nakagawa et al., 2005) or anti-PSD-95 monoclonal antibody (1:200, clone K28/43) with secondary antibodies: anti-rabbit IgG conjugated with Alexa488 or anti-mouse IgG conjugated with Alexa568 (1:200, Clontech). Images were recorded using CCD camera (Hamamatsu photonics, ORCA) mounted on a spinning disk confocal fluorescent microscope (Olympus, 60x objective lens).

Electrophysiology

Voltage clamp recordings were performed on outside-out patches from HEK293T cells as described previously (Rossmann et al., 2011). Briefly, cells were transfected with GluA2-Q (flip) and GSG1L plasmids (DNA ratio 1:2) or GluA2-Q (flip) alone. Current responses of outside-out patches (voltage-clamped at -60 mV) were elicited by fast application of 10 mM L-glutamate via a Θ-tube and recorded using Axopatch-1D amplifier, Digidata1322 interface and pClamp p.2 software (Molecular Devices). The rate of receptor desensitization was measured

by fitting the current decay during a 100 ms application of L-glutamate with a double-exponential function. Recovery from desensitization was assessed using a two-pulse protocol where a 100 ms agonist application is followed by a 10 ms application in increasing intervals. The relative peaks of the response to the second pulse were then plotted against time elapsed from the first pulse and fitted with a single-exponential function.

Immunohistochemistry

Six week old rat (male) was anesthetized and perfusion fixation was conducted using 4% paraformaldehyde in normal rat Ringer solution. Brain was dissected into small pieces containing the region of interest and further cryo-protected by immersing into a sequence of 0.1 M phosphate buffer pH 7.4 containing ascending concentration of sucrose (ranging from 4, 10, 15 and 20%). The tissues were quick frozen using liquid ethane and sectioned using cryostat (Leica CM1850). Sections (40 µm) were mounted on slide glass, blocked using 0.1M phosphate buffer pH 7.4, 4% BSA, and stained using the primary antibody (anti-GSG1L, Lp1 and anti-PSD95, clone K28/43) at 10µg/ml in 0.1M phosphate buffer pH 7.4, 0.2% TritonX-100, 0.2% BSA (at 4^{o}C, overnight). Preimmune serum was used such that the IgG concentration will be equivalent to the anti-GSG1L. Alexa488 and 568 conjugated anti-rabbit IgG (Invitrogen) was used as secondary antibody (for 1 hr at room temperature). Images were recorded using Olympus FV1000 confocal microscopy (objective lens 20x and 60x).

3. Supplementary text.

Candidates for future discovery

Many proteins that were previously reported to play roles in neurological and psychiatric disorders and synaptic plasticity were found in our interactome. For example, in Table S1, IL1RAPL1 known as X-linked interleukin-1 receptor accessory protein-like 1 precursor was found together with its ligand RPTPdelta in the AMPA-R preparation (Yoshida et al., 2011).

Fewer interacting partners are known for KA-Rs compared to AMPA-Rs. Neto1-2, MAGUK scaffolds, and Kelch interact with and modulate KA-R function (Garcia et al., 1998; Marshall et al., 2011; Zhang et al., 2009). Consistently, these proteins were among the most abundant hits in our KA-R interctome (Fig 1A2, and Table 1). The actin based motor myosin XVIII (Foth et al., 2006) was also represented abundantly in the KA-R interactome. Given the localization of KA-Rs in sophisticated actin rich spine architectures in CA3 pyramidal cells, myosin XVIII may potentially be an important candidate. Interestingly, myosin XVIII has a PDZ domain next to the motor domain. The C-termini of KA-R subunits are known PDZ ligands and thus it will be interesting to test if interactions exist between the PDZ domains of myosin XVIII and KA-Rs.

The secreted pentraxins are known interactors of AMPA-Rs (O'Brien et al., 1999; Sia et al., 2007). However, our results indicate that they are more abundantly found with KA-Rs, indicating the possibility of pentraxin function in modulating KA-R function. We also find significant peptide counts of neuronal secreted protein Olfm specifically found with AMPA-Rs.

4. References of the known and candidate interactors in Table1.

A. Known interactors

TARPs, CNIH, CKAMP44, Netos are reviewed in (Jackson and Nicoll, 2011)

PSD-95, PSD-93, SAP97, SAP-102, GRIPs are reviewed in (Kim and Sheng, 2004)

Protein 4.1 (Shen et al., 2000)

AP-2, NSF (Lee et al., 2002)

Kelch (Salinas et al., 2006)

B. Candidate interactors

MAGUK p55, CASK, Lin7 are major synaptic scaffold protein and is justifiable as potential indirect interactors (Kim and Sheng, 2004).

Liprin interacts with AMPA-R via GRIP (Wyszynski et al., 2002) and is an indirect interactor.

NGL-3 (LRRC4b) binds directly to PSD-95 (Woo et al., 2009). Because PSD-95 binds to stg/TARPs (Bats et al., 2007; Schnell et al., 2002), which binds directly to GluA2, NGL-3 is a candidate indirect interactor.

Leucine-rich transmembrane protein, LRRTM2 interacts with AMPA-Rs (de Wit et al., 2009) and is part of a large protein family. It is then plausible that members of the LRRTM family identified in our interactomes would be prime candidates for further experimental verification. Those include proteins listed as LRRC family in Table 1.

FLRT-2 and Latrophilin functionally interact with AMPA-Rs (O'Sullivan et al., 2012).

Neurexin (Nrxn) and neuroligin (Nlgn) form complex and interacts with PSD-95 (Irie et al., 1997), while PSD-95 interacts with stargazing/TARPs (Bats et al., 2007; Schnell et al., 2002).

Eph receptors and their ligands ephrins functionally intersect with AMPA-Rs in synapses (Ethell et al., 2001) and were detected with AMPA-Rs.

Myosin18 was the most abundantly found protein in the GluK2 interactome and thus was included in Table 1 as candidate.

DHHC5 interacts with GRIP (Thomas et al., 2012), which interacts with GluA2 (Dong et al., 1997), and thus considered as an indirect interactor.

RTRT family is related to LAR which binds to liprin (Dunah et al., 2005). LAR is also a receptor for NGL-3 (Woo et al., 2009), which is described above.

Shisa-6 belongs to the Shisa family (Pei and Grishin, 2012) that includes the well established AMPA-R binding partner CKAMP44 (von Engelhardt et al., 2010).

Pentraxins are described as AMPA-R binding proteins in the literature (O'Brien et al., 1999; Sia et al., 2007). Interestingly we find these proteins associating preferentially with kainite receptors.

SynDIG1 is a known interactor of AMPA-R and belongs to the PRRT family of proteins. PRRT 1 (NG5 and synDIG4), and pancortin-3 (Olfm1) are known to co-purify with AMPA-Rs in the supplementary figure of (von Engelhardt et al., 2010). Our study extends the interactome by identifying their homologues such as PRRT 2 and Olfm-3 (Table1).

5. References

Bats, C., Groc, L., and Choquet, D. (2007). The interaction between Stargazin and PSD-95 regulates AMPA receptor surface trafficking. Neuron *53*, 719-734.

Cociorva, D., D, L.T., and Yates, J.R. (2007). Validation of tandem mass spectrometry database search results using DTASelect. Curr Protoc Bioinformatics *Chapter 13*, Unit 13 14.

de Wit, J., Sylwestrak, E., O'Sullivan, M.L., Otto, S., Tiglio, K., Savas, J.N., Yates, J.R., 3rd, Comoletti, D., Taylor, P., and Ghosh, A. (2009). LRRTM2 interacts with Neurexin1 and regulates excitatory synapse formation. Neuron *64*, 799-806.

Dong, H., O'Brien, R.J., Fung, E.T., Lanahan, A.A., Worley, P.F., and Huganir, R.L. (1997). GRIP: a synaptic PDZ domain-containing protein that interacts with AMPA receptors. Nature *386*, 279-284.

Dunah, A.W., Hueske, E., Wyszynski, M., Hoogenraad, C.C., Jaworski, J., Pak, D.T., Simonetta, A., Liu, G., and Sheng, M. (2005). LAR receptor protein tyrosine phosphatases in the development and maintenance of excitatory synapses. Nat Neurosci *8*, 458-467.

Eng J, M.A., Yates JR., 3rd (1994). J Am Soc Mass Spectrom. J Am Soc Mass Spectrom *5*, 976-989.

Ethell, I.M., Irie, F., Kalo, M.S., Couchman, J.R., Pasquale, E.B., and Yamaguchi, Y. (2001). EphB/syndecan-2 signaling in dendritic spine morphogenesis. Neuron *31*, 1001-1013.

Farina, A.N., Blain, K.Y., Maruo, T., Kwiatkowski, W., Choe, S., and Nakagawa, T. (2011). Separation of Domain Contacts Is Required for Heterotetrameric Assembly of Functional NMDA Receptors. J Neurosci *31*, 3565-3579.

Foth, B.J., Goedecke, M.C., and Soldati, D. (2006). New insights into myosin evolution and classification. Proc Natl Acad Sci U S A *103*, 3681-3686.

Garcia, E.P., Mehta, S., Blair, L.A., Wells, D.G., Shang, J., Fukushima, T., Fallon, J.R., Garner, C.C., and Marshall, J. (1998). SAP90 binds and clusters kainate receptors causing incomplete desensitization. Neuron *21*, 727-739.

Irie, M., Hata, Y., Takeuchi, M., Ichtchenko, K., Toyoda, A., Hirao, K., Takai, Y., Rosahl, T.W., and Sudhof, T.C. (1997). Binding of neuroligins to PSD-95. Science *277*, 1511-1515.

Jackson, A.C., and Nicoll, R.A. (2011). The expanding social network of ionotropic glutamate receptors: TARPs and other transmembrane auxiliary subunits. Neuron *70*, 178-199.

Kim, E., and Sheng, M. (2004). PDZ domain proteins of synapses. Nat Rev Neurosci *5*, 771-781.

Lee, S.H., Liu, L., Wang, Y.T., and Sheng, M. (2002). Clathrin adaptor AP2 and NSF interact with overlapping sites of GluR2 and play distinct roles in AMPA receptor trafficking and hippocampal LTD. Neuron *36*, 661-674.

Marshall, J., Blair, L.A., and Singer, J.D. (2011). BTB-Kelch proteins and ubiquitination of kainate receptors. Adv Exp Med Biol *717*, 115-125.

McDonald, W.H., Tabb, D.L., Sadygov, R.G., MacCoss, M.J., Venable, J., Graumann, J., Johnson, J.R., Cociorva, D., and Yates, J.R., 3rd (2004). MS1, MS2, and SQT-three unified, compact, and easily parsed file formats for the

storage of shotgun proteomic spectra and identifications. Rapid Commun Mass Spectrom *18*, 2162-2168.
Nakagawa, T., Cheng, Y., Ramm, E., Sheng, M., and Walz, T. (2005). Structure and different conformational states of native AMPA receptor complexes. Nature *433*, 545-549.
O'Brien, R.J., Xu, D., Petralia, R.S., Steward, O., Huganir, R.L., and Worley, P. (1999). Synaptic clustering of AMPA receptors by the extracellular immediate-early gene product Narp. Neuron *23*, 309-323.
O'Sullivan, M.L., de Wit, J., Savas, J.N., Comoletti, D., Otto-Hitt, S., Yates, J.R., 3rd, and Ghosh, A. (2012). FLRT Proteins Are Endogenous Latrophilin Ligands and Regulate Excitatory Synapse Development. Neuron *73*, 903-910.
Pei, J., and Grishin, N.V. (2012). Unexpected diversity in Shisa-like proteins suggests the importance of their roles as transmembrane adaptors. Cell Signal *24*, 758-769.
Peng, J., Elias, J.E., Thoreen, C.C., Licklider, L.J., and Gygi, S.P. (2003). Evaluation of multidimensional chromatography coupled with tandem mass spectrometry (LC/LC-MS/MS) for large-scale protein analysis: the yeast proteome. J Proteome Res *2*, 43-50.
Rossmann, M., Sukumaran, M., Penn, A.C., Veprintsev, D.B., Babu, M.M., and Greger, I.H. (2011). Subunit-selective N-terminal domain associations organize the formation of AMPA receptor heteromers. Embo J *30*, 959-971.
Sadygov, R.G., Eng, J., Durr, E., Saraf, A., McDonald, H., MacCoss, M.J., and Yates, J.R., 3rd (2002). Code developments to improve the efficiency of automated MS/MS spectra interpretation. J Proteome Res *1*, 211-215.
Salinas, G.D., Blair, L.A., Needleman, L.A., Gonzales, J.D., Chen, Y., Li, M., Singer, J.D., and Marshall, J. (2006). Actinfilin is a Cul3 substrate adaptor, linking GluR6 kainate receptor subunits to the ubiquitin-proteasome pathway. J Biol Chem *281*, 40164-40173.
Schnell, E., Sizemore, M., Karimzadegan, S., Chen, L., Bredt, D.S., and Nicoll, R.A. (2002). Direct interactions between PSD-95 and stargazin control synaptic AMPA receptor number. Proc Natl Acad Sci U S A *99*, 13902-13907.
Shanks, N.F., Maruo, T., Farina, A.N., Ellisman, M.H., and Nakagawa, T. (2010). Contribution of the global subunit structure and stargazin on the maturation of AMPA receptors. J Neurosci *30*, 2728-2740.
Shen, L., Liang, F., Walensky, L.D., and Huganir, R.L. (2000). Regulation of AMPA receptor GluR1 subunit surface expression by a 4. 1N-linked actin cytoskeletal association. J Neurosci *20*, 7932-7940.
Sia, G.M., Beique, J.C., Rumbaugh, G., Cho, R., Worley, P.F., and Huganir, R.L. (2007). Interaction of the N-terminal domain of the AMPA receptor GluR4 subunit with the neuronal pentraxin NP1 mediates GluR4 synaptic recruitment. Neuron *55*, 87-102.
Tabb, D.L., McDonald, W.H., and Yates, J.R., 3rd (2002). DTASelect and Contrast: tools for assembling and comparing protein identifications from shotgun proteomics. J Proteome Res *1*, 21-26.

Thomas, G.M., Hayashi, T., Chiu, S.L., Chen, C.M., and Huganir, R.L. (2012). Palmitoylation by DHHC5/8 targets GRIP1 to dendritic endosomes to regulate AMPA-R trafficking. Neuron *73*, 482-496.
von Engelhardt, J., Mack, V., Sprengel, R., Kavenstock, N., Li, K.W., Stern-Bach, Y., Smit, A.B., Seeburg, P.H., and Monyer, H. (2010). CKAMP44: a brain-specific protein attenuating short-term synaptic plasticity in the dentate gyrus. Science *327*, 1518-1522.
Washburn, M.P., Wolters, D., and Yates, J.R., 3rd (2001). Large-scale analysis of the yeast proteome by multidimensional protein identification technology. Nat Biotechnol *19*, 242-247.
Woo, J., Kwon, S.K., Choi, S., Kim, S., Lee, J.R., Dunah, A.W., Sheng, M., and Kim, E. (2009). Trans-synaptic adhesion between NGL-3 and LAR regulates the formation of excitatory synapses. Nat Neurosci *12*, 428-437.
Wyszynski, M., Kim, E., Dunah, A.W., Passafaro, M., Valtschanoff, J.G., Serra-Pages, C., Streuli, M., Weinberg, R.J., and Sheng, M. (2002). Interaction between GRIP and Liprin-alpha/SYD2 Is Required for AMPA Receptor Targeting. Neuron *34*, 39-52.
Yoshida, T., Yasumura, M., Uemura, T., Lee, S.J., Ra, M., Taguchi, R., Iwakura, Y., and Mishina, M. (2011). IL-1 receptor accessory protein-like 1 associated with mental retardation and autism mediates synapse formation by trans-synaptic interaction with protein tyrosine phosphatase delta. J Neurosci *31*, 13485-13499.
Zhang, W., St-Gelais, F., Grabner, C.P., Trinidad, J.C., Sumioka, A., Morimoto-Tomita, M., Kim, K.S., Straub, C., Burlingame, A.L., Howe, J.R., and Tomita, S. (2009). A transmembrane accessory subunit that modulates kainate-type glutamate receptors. Neuron *61*, 385-396.

Supplemental Figure S1

A

Accession	Spec. Count	Pep. Count	% AA	Description
IPI00030882	1262	110	63.3	GRIA2 Isoform Flop of Glutamate receptor 2
IPI00152159	3	3	11.2	GSG1L Isoform 1 of Germ cell-specific gene 1-like protein
IPI00892819	3	3	13.9	GSG1L Isoform 2 of Germ cell-specific gene 1-like protein

B

Sequence	Spec. Count	Confidence (%)	Scan	Charge	Xcorr	DeltCN	ppm
R.NFHTGIWYSCEEELSGLGEK.C	1	100	13673	2	5.5248	0.5601	-2
R.NFHTGIWYSCEEELSGLGEK.C	1	100	13683	3	5.1518	0.4791	-0.4
K.VFEQGYREEPTFIDPEAIK.Y	1	98.6	9509	3	2.3175	0.2096	1.2

C

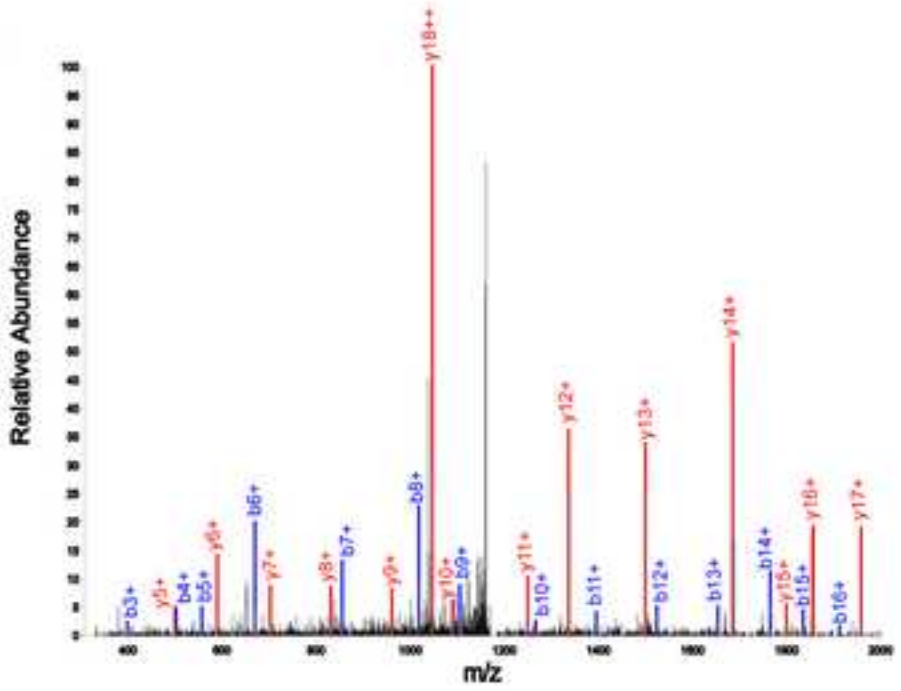

D

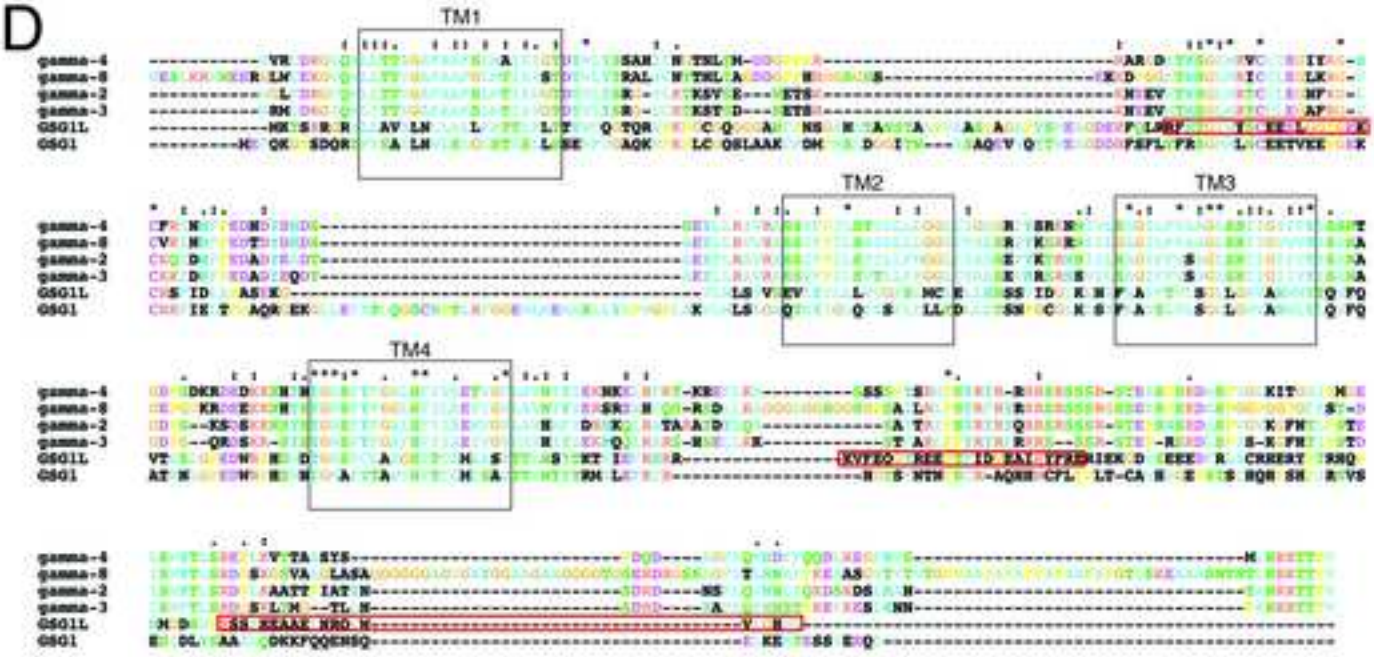

Supplementary Figure S1

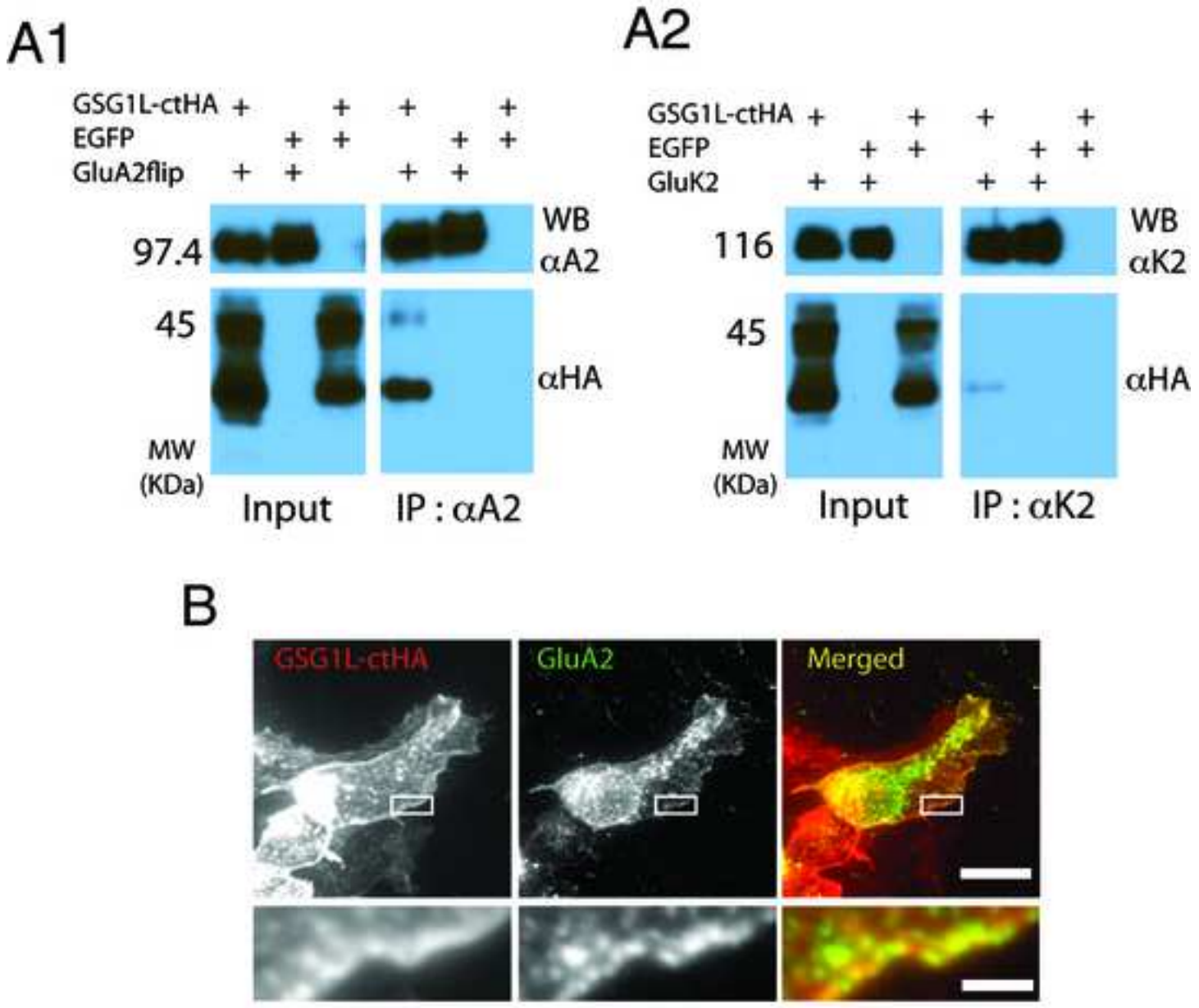

Supplementary Figure S2

Supplemental Figure S3

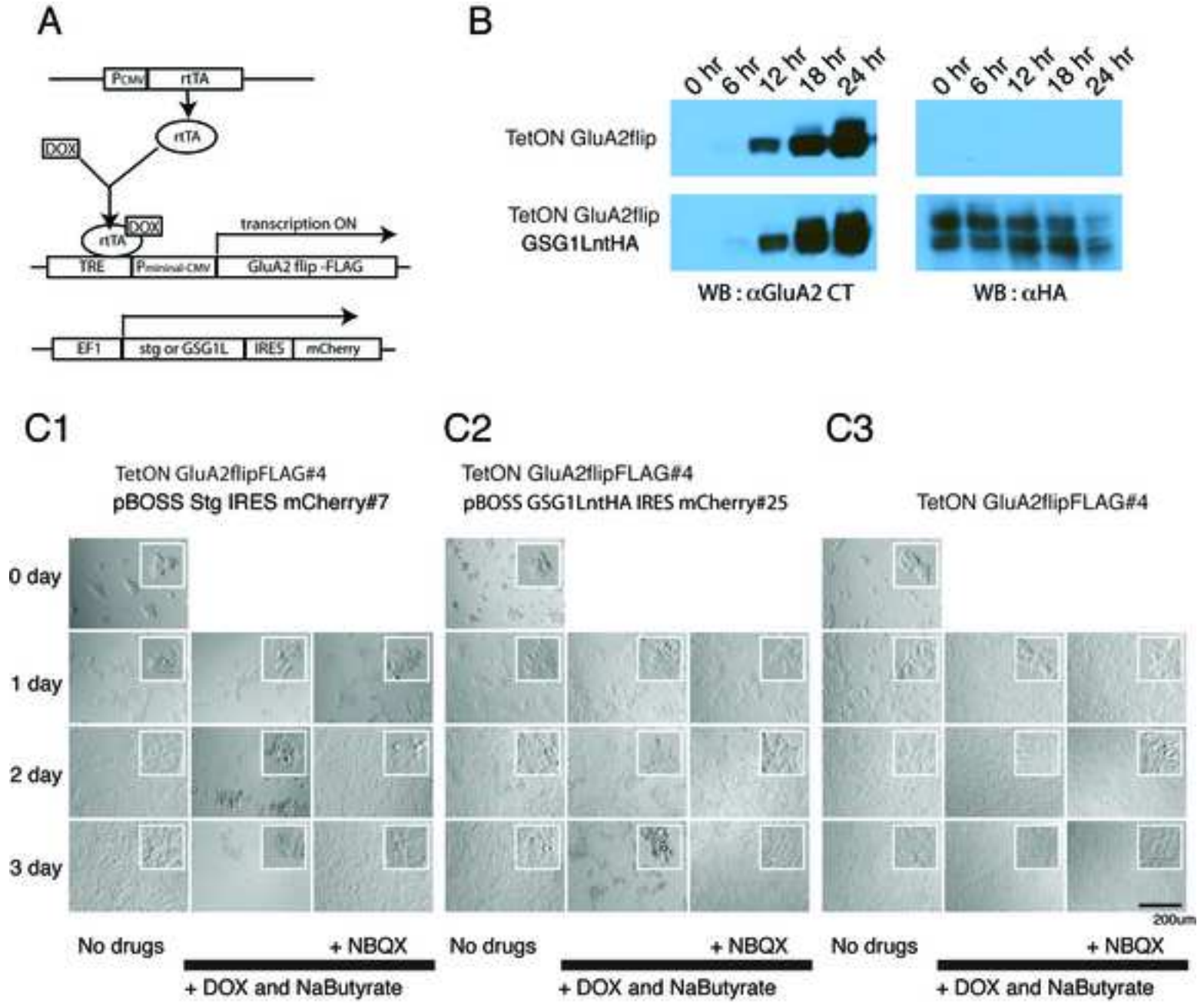

Supplementary Figure S3